

Eribulin mesylate exerts antitumor effects via CD103

Kazumasa Oya^a, Yoshiyuki Nakamura^a, Rei Watanabe^b, Ryota Tanaka^a, Yuki Ichimura^a, Noriko Kubota^a, Yutaka Matsumura^b, Hideaki Tahara^{c,d}, Naoko Okiyama^e, Manabu Fujimoto^b, Toshifumi Nomura^a, and Yasuhiro Fujisawa^a

^aThe Department of Dermatology, Faculty of Medicine, University of Tsukuba, Tsukuba, Japan; ^bThe Department of Dermatology, Graduate School of Medicine, Osaka University, Osaka, Japan; ^cProject Division of Cancer Biomolecular Therapy, Institute of Medical Science, The University of Tokyo, Tokyo, Japan; ^dDepartment of Cancer Drug Discovery and Development, Osaka International Cancer Center, Osaka, Japan; ^eDepartment of Dermatology, Graduate School of Medical and Dental Sciences, Tokyo Medical and Dental University, Tokyo, Japan

ABSTRACT

Eribulin mesylate (ERB) is a synthetic analog of halichondrin B, inhibiting tumor cell growth by disrupting microtubule function. Recently, anticancer drugs have been shown to not only act directly on tumor cells but also to exert antitumor effects by modifying the tumor environment. Although ERB has also been speculated to modify the tumor microenvironment including the immune response to tumors, the precise mechanism remains unclear. In our study, ERB suppressed the tumor growth of MC38 colon cancer in wildtype mice, whereas ERB failed to inhibit the tumor growth in Rag1-deficient mice which lack both B and T cells. Moreover, depletion of either CD4⁺ or CD8⁺ T cells abrogated the antitumor effect of ERB, indicating that both CD4⁺ and CD8⁺ T cells play an important role in ERB-induced antitumor effects. Furthermore, ERB treatment increased the number of tumor infiltrating lymphocytes (TILs) as well as the expression of activation markers (CD38 and CD69), immune checkpoint molecules (LAG3, TIGIT and Tim3) and cytotoxic molecules (granzyme B and perforin) in TILs. ERB upregulated E-cadherin expression in MC38. CD103 is a ligand of E-cadherin and induces T-cell activation. ERB increased the proportion of CD103⁺ cells in both CD4⁺ and CD8⁺ TILs. The ERB-induced antitumor effect with the increased TIL number and the increased expression of activation markers, inhibitory checkpoint molecules and cytotoxic molecules in TILs was abrogated in CD103-deficient mice. Collectively, these results suggest that ERB exerts antitumor effects by upregulation of E-cadherin expression in tumor cells and subsequent activation of CD103⁺ TILs.

ARTICLE HISTORY

Received 18 December 2022
Revised 30 April 2023
Accepted 23 May 2023

KEYWORDS



antitumor effect; CD103; eribulin mesylate; immune checkpoint; resident memory T cells


1. Introduction

Eribulin mesylate (ERB) is a synthetic analog of halichondrin B, a natural product extracted from the marine sponge *Halichondria okadai*^{1,2}. ERB exerts potent antitumor effects against various tumor cells both *in vitro* and *in vivo*^{3–5}. ERB improved overall survival (OS) not only in advanced breast cancer patients previously treated with an anthracycline and taxanes⁶, but also in advanced liposarcoma patients previously treated with anthracycline⁷. ERB was also effective in patients with advanced cutaneous angiosarcoma, who were previously treated with taxanes⁸. ERB prevents the elongation of microtubules and inhibits mitosis by binding to the plus ends of microtubules². In addition, previous studies have shown that ERB increased the expression of epithelial markers such as E-cadherin and reduced the expression of mesenchymal markers such as N-cadherin and vimentin, leading to a reversal of epithelial-mesenchymal transition (EMT)⁵. This reversal of EMT is also considered to have important roles in ERB-induced antitumor effects^{2,9}. Moreover, recent studies suggest that ERB may also influence the immune response to tumors. In a study using human cancer xenograft models, ERB

increased the number of CD11b⁺ cells in the tumor and depletion of NK cells attenuated the ERB-induced antitumor effect⁹. Goto et al revealed that advanced breast cancer patients with an increased number of CD8⁺ T cells and a decreased number of regulatory T cells responded well to ERB therapy¹⁰. Another clinical study showed that breast cancer patients with high tumor-infiltrating lymphocytes (TILs) had longer disease-free survival than those with low TILs when treated with ERB¹¹. Although these findings suggest that ERB might exert immunomodulatory antitumor effects, the precise mechanism remains unclear.

CD103 (integrin α E) is primarily expressed on tissue-resident memory T cells, which play vital roles in tumor immunity¹². CD103 forms the complete heterodimeric integrin molecule α E β 7 with integrin β 7 and binds to E-cadherin, which is commonly expressed on the surface of epithelial cells¹³. CD103 on the surface of T cells binds to cancer cells expressing E-cadherin¹⁴, resulting in activation of the T cells¹⁵. A recent meta-analysis demonstrated that solid tumors positive for CD103⁺ immune cells were associated with longer OS¹². Consistently, a large number of CD103⁺ TILs has also been

CONTACT Yoshiyuki Nakamura  [ynakamura-tuk@umin.ac.jp](mailto:yinakamura-tuk@umin.ac.jp) 

 Supplemental data for this article can be accessed online at <https://doi.org/10.1080/2162402X.2023.2218782>

© 2023 The Author(s). Published with license by Taylor & Francis Group, LLC.

This is an Open Access article distributed under the terms of the Creative Commons Attribution-NonCommercial License (<http://creativecommons.org/licenses/by-nc/4.0/>), which permits unrestricted non-commercial use, distribution, and reproduction in any medium, provided the original work is properly cited. The terms on which this article has been published allow the posting of the Accepted Manuscript in a repository by the author(s) or with their consent.

reported to be correlated with improved prognosis for patients suffering from non – small cell lung carcinoma¹⁶ or ovarian cancer¹⁷. Thus, CD103⁺ T cells have been recognized to represent crucial components in tumor immune surveillance. Since ERB is known to enhance E-cadherin expression in tumor cells⁵, we hypothesized that an increased expression of E-cadherin by ERB could exert antitumor effects by activation of CD103⁺ T cells. In this study, we aim to elucidate novel mechanisms of ERB-induced antitumor effects through regulation of the immune response to tumors.

2. Material and methods

2.1. Mice

C57BL/6J and Balb/c mice raised under specific pathogen-free conditions were purchased from CLEA Japan. Rag1-deficient mice, μ MT mice, and CD103-deficient mice were purchased from the Jackson Laboratory (Bar Harbor, ME, USA). Mice between 8 and 12 weeks of age were used for the experiments. All the experiments were performed in accordance with the guidelines of the animal ethics committee of the University of Tsukuba Animal Research Center (permission number: #22–237).

2.2. Cell lines

B16F10 (mouse melanoma; from the Cell Resource Center for Biomedical Research Institute of Development, Japan), MC38 (mouse colon carcinoma; kindly provided by Dr. H. Tahara, The Institute of Medical Science, University of Tokyo), LLC (mouse lung carcinoma; kindly provided by Dr. M. Sakata-Yanagimoto, Department of Hematology, University of Tsukuba) and MB49 (mouse bladder carcinoma; kindly provided by Dr. W.T. Godbey, Department of Chemical & Biomolecular Engineering, Tulane University) were cultivated in DMEM (Thermo Fisher) with 100 mM sodium pyruvate (Wako), 1% MEM nonessential amino acids solution (Wako), and 100 mM L-alanyl-L-glutamine (Wako), 4T1 (American Type Culture Collection) was cultivated in RPMI 1640 (Wako) at 37°C under 5% CO₂. These media were supplemented with 10% FBS and 1% penicillin-streptomycin (Wako),

2.3. Murine tumor model

Tumor cells were subcutaneously injected into mice and tumor growth was analyzed as described previously¹⁸. Briefly, we intradermally injected 3×10^5 cells of B16F10, 1×10^6 of LLC, MB49, and 4T1, or 2×10^6 cells of MC38 cells into the back of the mice. After inoculation of the mice, the diameters of the tumors were measured with a caliper and the tumor volume was determined according to the following formula: tumor volume (mm³) = (length) \times (width)² \times 0.5. Regarding survival analysis, the mice were euthanized when the tumor volume reached 4000 mm³, and the time for tumor volume to reach this endpoint was evaluated. ERB was kindly gifted by Eisai Co., Ltd and 10 μ g of this reagent was intravenously administered to mice on day 2 after tumor inoculation. Anti-PD-1

antibody (RMP1–14) was purchased from Bio X Cell (Lebanon). The mice were given intraperitoneal injections of anti-PD-1 antibody (200 μ g/mouse) every 4 days from day 4 to day 16. All the experiments were performed in accordance with the guidelines of the animal ethics committee of the University of Tsukuba Animal Research Center (permission number: #22–237).

2.4. Histopathologic analysis

Tissue blocks were fixed in 10% formalin. After paraffin embedding, 3- μ m sections were subjected to staining. For the cell number counts, 5 randomly selected sites at 400 \times magnification were evaluated by use of light microscopy. For immuno-histochemistry of CD4 or CD8, samples were deparaffinized in xylene and re-hydrated before antigen retrieval by boiling in citrate buffer (0.01 M citrate containing 0.5% Tween 20, pH 6.0). The sections were incubated in 10% BSA in PBS for 1 hour and then stained with rat anti-CD4 antibody (4SM95, 1:500 dilution; Thermo Fisher) and anti-CD8 antibody (4SM15, 1:500 dilution; Thermo Fisher) overnight at 4°C, followed by biotinylated anti-rat IgG antibody (1:500; Vector Laboratories) and Vectastain ABC reagent (Vector Laboratories) at room temperature for 60 minutes and 30 minutes, respectively. Finally, the sections were stained by the use of a DAB Peroxidase Substrate Kit (Vector Laboratories) before imaging.

2.5. In vitro assay

Splenocytes or tumor cells were seeded at 1.5×10^6 cells/well (splenocytes) or 1.0×10^6 cells/well (tumor cells) in a 6-well plate in complete RPMI1640 (splenocytes) or DMEM (tumor cells) with various concentrations of ERB as indicated in the figure legends or dimethyl sulfoxide as the control. After stimulation for the indicated time, the cells were used for counting living cell numbers, flow cytometric analyses, or analyses of the quantitative reverse transcription-polymerase chain reaction (qRT-PCR).

2.6. Cell isolation

For cell isolation, whole tumors were minced with scissors and digested in complete medium with 2 mg/mL crude collagenase (Wako) and 2 KU/mL DNase I deoxyribonuclease I from bovine pancreas (Sigma) with a GentleMACS tissue processor (Miltenyi Biotec). The digested tissue was cultured at 37°C for 30 minutes to prepare the tumor cell suspension.

2.7. Flow cytometric analysis

Isolated cells were incubated in a FACS staining buffer (PBS containing 5% BSA and 0.01% NaN₃) with FcR Blocking Reagent (Miltenyi Biotec). The cells were then stained with antibodies. The following antibodies were purchased from BioLegend: anti-CD4 (RM4–5), anti-CD8 α (53–6.7), anti-CD11b (M1/70), anti-CD11c (N418), anti-CD19 (6D5), anti-

CD45.2 (104), anti-CD38 (90), anti-CD69 (H1.2F3), anti-PD-1 (29F.1A12), anti-LAG3 (C9B7W), anti-TIGIT (1G9), anti-Tim3 (RMT3-23), anti-CD103 (2E7), anti-E-cadherin (DECMA-1), anti-granzyme B (QA16A02), anti-perforin (S16009A), anti-CD25 (PC61) mAbs. Anti-CD4 (GK1.5), anti-CD3 ϵ (145-2C11) and anti-FoxP3 (FJK-16s) mAbs were purchased from Thermo Fisher. Dead cells were detected by the 7-AAD Viability Staining Solution (Thermo Fisher) or a Zombie Fixable Viability Kit (BioLegend). Flow cytometry was performed on a Beckman Coulter Gallios instrument, and the data were analyzed using Kaluza Flow Analysis software (Beckman Coulter).

2.8. qRT-PCR

Total RNA was isolated by the use of Trizol Reagent (Invitrogen). Analyses of qRT-PCR were performed on the QuantStudio™ 5 Real-Time PCR System with PrimeTime® Gene Expression Master Mix and Prime Time qPCR pre-designed primers (Integrated DNA Technologies). The mRNA level of each gene was normalized to that of GAPDH. The primer used was as follows: E-cadherin: Mm.PT.58.41847659.

2.9. In vivo depletion of CD4⁺ or CD8⁺ T cells

To deplete T cells from mice, purified anti-CD4 monoclonal antibodies (GK1.5) or anti-CD8 monoclonal antibodies (53.67.2) were used. The mice were intraperitoneally injected with 250 μ g of anti-CD4 antibody or anti-CD8 antibody, on three consecutive days from day -3 to -1 before tumor inoculation and every 3 days after tumor inoculation (CD4), or on five consecutive days from day -5 to -1 before tumor inoculation and every 4 days after tumor inoculation (CD8), respectively.

2.10. Measurement of high mobility group box 1 (HMGB1) and extracellular ATP

MC38 cells were seeded at 1.0×10^4 cells/well in a 96-well plate in complete DMEM with various concentrations of ERB as indicated in the figure legends or dimethyl sulfoxide as the control. After 24 (ATP) or 48 (HMGB1) hours of culture, ATP and HMGB1 in the culture supernatants were analyzed with the RealTime-Glo Extracellular ATP Assay Kit (Promega) or Lumit HMGB1 Immunoassay (Promega) according to the manufacturer's instructions.

2.11. Statistical analysis

For analyzing the survival data, the Log-rank test was used. Mann - Whitney U test was used for analysis of the other experiments. Throughout the analysis, probability values less than 0.05 were considered significant. The statistical tests were 2-sided and carried out using Prism version 9 (GraphPad Software).

3. Results

3.1. T cells are indispensable for the ERB-induced antitumor effect

We tested the antitumor effect of ERB using 5 different tumor cell lines: B16F10, MC38, LLC, MB49 and 4T1. To analyze the direct cytotoxic effect of ERB, we evaluated the number of living cells 4 days after the addition of ERB *in vitro*. Although ERB at up to 1.0 nM did not affect the number of living cells, ERB at 10 nM significantly reduced the number of living cells in all the cell lines (Figure 1a, Supplementary Figure S1A). Next, to evaluate the antitumor effect of ERB in the tumor mouse model, ERB was intravenously administered 2 days after tumor cells were inoculated. We found that ERB significantly inhibited the growth of MC38, LLC and MB49, whereas ERB failed to suppress tumor growth of B16F10 and 4T1 (Figure 1b, Supplementary Figure S1B). In addition, ERB treatment prolonged survival in MC38-implanted mice (Figure 1c). Given that B16F10 and 4T1 are less immunogenic compared with the other cell lines^{18,19}, the antitumor effect of ERB *in vivo* may be dependent on tumor immunogenicity. To focus on the underlying antitumor effect of ERB via immune systems rather than on the direct cytotoxic effects, we selected MC38 for further experiments because MC38 was more resistant to a high concentration (10 nM) of ERB *in vitro* when compared with LLC or MB49. An *in vitro* analysis of the immunogenic cell death (ICD) activity (which plays an important role in cancer therapy²⁰) revealed that ERB treatment increased extracellular ATP and HMGB1 levels in MC38, suggesting ERB-induced ICD induction (Supplementary Figure S1C, D). Next, to clarify the role of adaptive immunity in the antitumor effect of ERB, we assessed the tumor growth of MC38 in Rag1-deficient mice (lacking both T and B cells) and in μ MT mice (lacking B cells). Whereas ERB failed to inhibit the tumor growth in Rag1-deficient mice (Figure 1d), ERB significantly inhibited the growth of tumor in μ MT mice similar to wildtype mice (Figure 1e). These results suggest that ERB-induced antitumor effect is dependent on T cells. Then, we also found that ERB failed to inhibit tumor growth in both mice with depletion of CD4⁺ T cells (Figure 1f) and those with depletion of CD8⁺ T cells (Figure 1g). These results indicate that both CD4⁺ and CD8⁺ T cells play critical roles in the ERB-induced antitumor effect.

3.2. ERB enhances the activation of both CD4⁺ and CD8⁺ T cells in the tumor

Since the ERB-induced antitumor effect was dependent on both CD4⁺ and CD8⁺ T cells, we evaluated the TIL number by immunohistochemical studies after ERB treatment. We found that the number of both CD4⁺ and CD8⁺ TILs was significantly increased by ERB treatment (Figure 2a), whereas ERB did not affect the proportion of regulatory T cells in the tumor (Supplementary Figure S2A). Next, we evaluated CD38 and CD69 (activation markers of T cells) by flow cytometric analysis, and found that the expressions of these molecules in both CD4⁺ and CD8⁺ TILs were significantly upregulated by ERB treatment (Figure 2b). Similarly, the expressions of

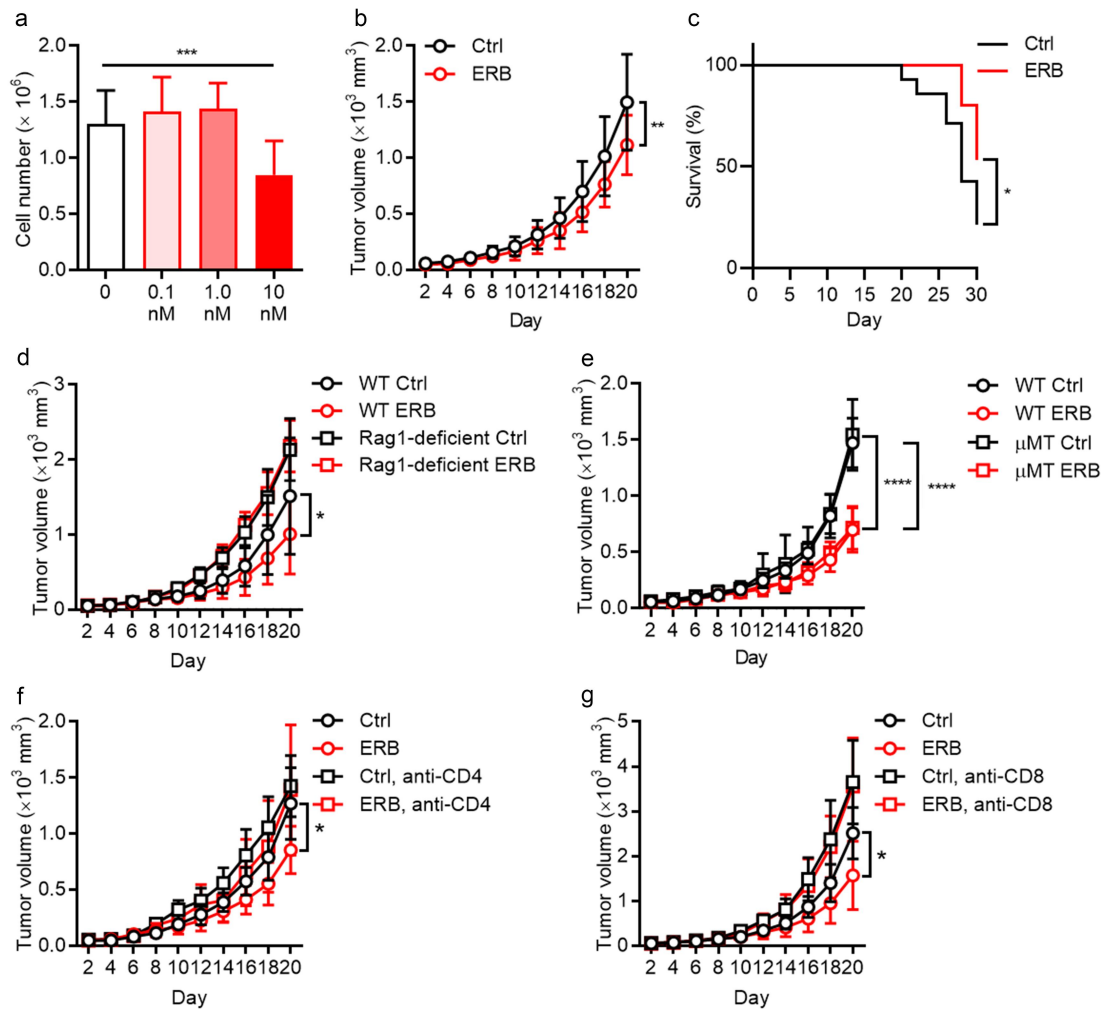


Figure 1. T cells are indispensable for the ERB-induced antitumor effect. Note: (A) The number of living cells stimulated with ERB at various concentrations for 4 days *in vitro* ($n = 10$ at 0 nM and $n = 12$ at 0.1–10 nM per group [MC38]). (B) Time course of the tumor volume after MC38 cells were intradermally inoculated into wildtype mice. ERB was intravenously administered to mice on day 2 ($n = 18$ in control group and $n = 17$ in ERB treatment group [MC38]). (C) Survival curves showing the survival percentage during the experiment ($n = 14$ in control, $n = 15$ in ERB group). (D, E) Time course of the tumor volume after MC38 cells were intradermally inoculated into Rag1-deficient mice (D) or μ MT mice (E) with ERB administration ([D] $n = 21$ in wildtype mice with no treatment, $n = 19$ in wildtype mice with ERB treatment, and $n = 12$ per group of Rag1-deficient mice. [E] $n = 11$ per group of wildtype mice, $n = 17$ in μ MT mice with no treatment and $n = 16$ in μ MT mice with ERB treatment). (F, G) Time course of the tumor volume after MC38 cells were intradermally inoculated into wildtype mice with CD4⁺ (F) or CD8⁺ cells (G) depletion ([F] $n = 7$ per group, and [G] $n = 11$ per group). Ctrl: control, ERB: eribulin mesylate. Error bars indicate ± 1 SD; * $p < 0.05$, ** $p < 0.01$, *** $p < 0.001$, **** $p < 0.0001$.

granzyme B (GZMB) and perforin (cytotoxic molecules) in both CD4⁺ and CD8⁺ TILs were increased by ERB treatment (Figure 2c). Since immune checkpoint molecules are also induced after T-cell activation^{21,22}, we also investigated their expression. Whereas PD-1 expression in both CD4⁺ and CD8⁺ T cells was comparable between control and ERB treatment groups (Supplementary Figure S2B), LAG3 expression in CD8⁺ TILs was upregulated by ERB treatment (Supplementary Figure S2B). Furthermore, the expression of TIGIT and Tim3 in both CD4⁺ and CD8⁺ TILs was significantly increased by ERB treatment (Supplementary Figure S2B). These results suggest that ERB activates both CD4⁺ and CD8⁺ TILs. Since ERB activates T cells, we also assessed the antitumor effect induced by the combination treatment of ERB with anti-PD-1 antibody. However, we found that the antitumor effect of the combination treatment was comparable to that of anti-PD-1 antibody monotherapy (Supplementary Figure S3).

3.3. ERB enhances E-cadherin expression in MC38, LLC, MB49, but not in B16F10 or 4T1

Since previous studies showed that ERB enhances the expression of E-cadherin in several tumor cells^{5,23}, we examined the expression of E-cadherin in MC38. We found that the mRNA expression of E-cadherin was enhanced in MC38 after ERB treatment *in vitro* (Figure 3a). The cell surface expression of E-cadherin in MC38 (Figure 3b), LLC and MB49 (Supplementary Figure S4A) cells was also increased after ERB stimulation in a dose-dependent manner, while the expression of E-cadherin in B16F10 and 4T1 was unchanged (Supplementary Figure S4A). Next, we evaluated the E-cadherin expression in tumors after ERB treatment in the murine tumor model. Consistent with the *in vitro* findings, ERB upregulated E-cadherin expression in MC38 (Figure 3c), LLC and MB49, but not in B16F10 or 4T1 (Supplementary Figure S4B).

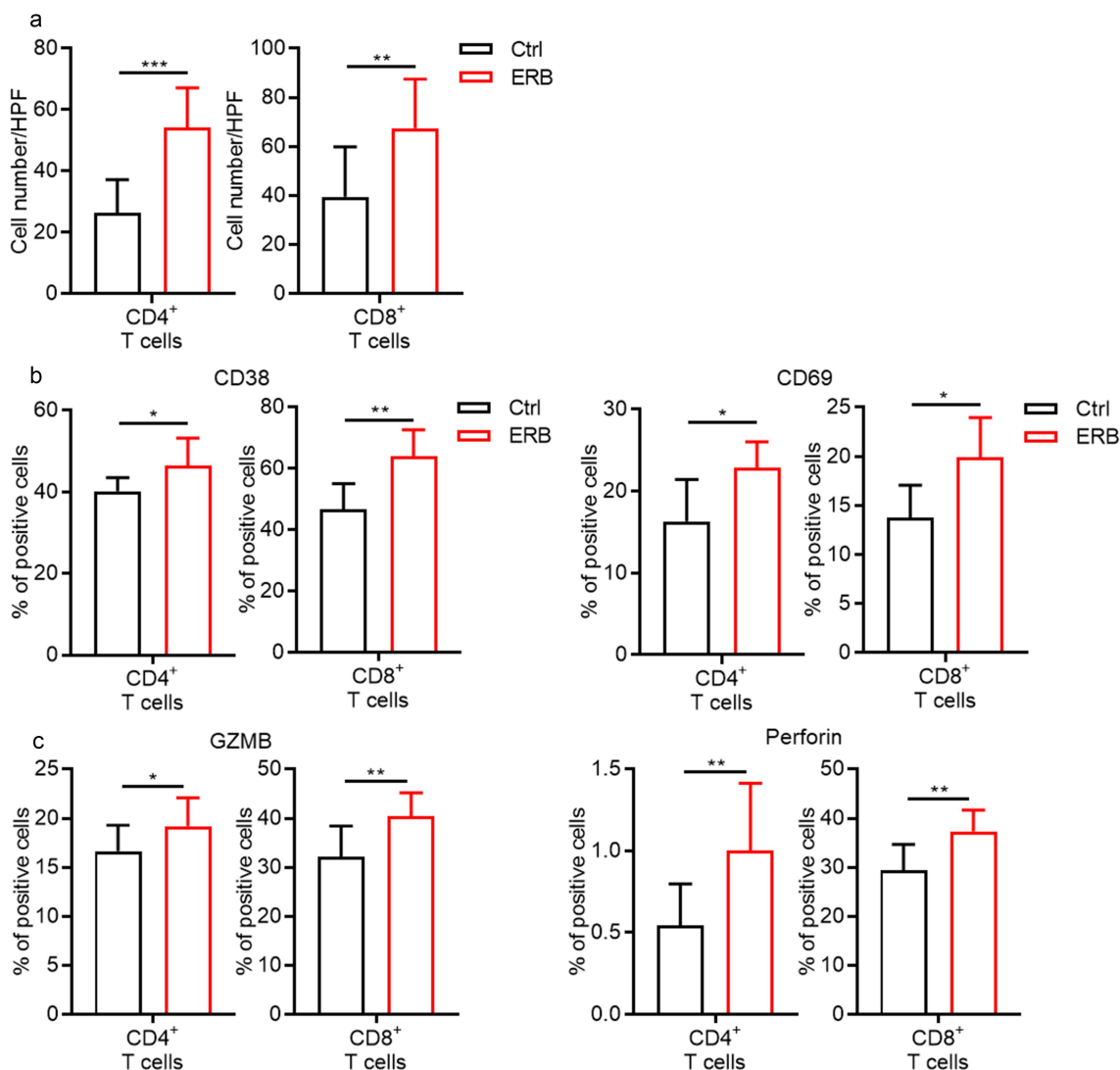


Figure 2. ERB enhances the activation of both CD4⁺ or CD8⁺ T cells in the tumor. Note: (A) The number of CD4⁺ and CD8⁺ T cells in the tumor 10 days after the inoculation of MC38 cells into wildtype mice ($n = 9$ per group). (B, C) Flow cytometric analysis of expression of CD38, CD69 (B), GZMB and perforin (C) in CD4⁺ and CD8⁺ T cells in tumors 7 days after tumor inoculation with ERB treatment on day 2 ($n = 6$ [B], and $n = 12$ [C] per group). Ctrl: control, ERB: eribulin mesylate, PD-1: programmed cell death-1, LAG3: lymphocyte activation gene 3, TIGIT: T-cell immunoreceptor with Ig and ITIM domains, Tim3: T-cell immunoglobulin and mucin domain 3, granzyme B: GZMB. Error bars indicate ± 1 SD; * $p < 0.05$, ** $p < 0.01$, *** $p < 0.001$.

3.4. The ERB-induced antitumor effect is dependent on CD103

Since CD103 is a ligand of E-cadherin¹³ and E-cadherin expression is upregulated by ERB in MC38, we speculated that ERB might affect CD103⁺ T-cell population. We found that ERB significantly increased the proportion of CD103⁺ cells in both CD4⁺ and CD8⁺ TILs (Figure 4a). However, ERB did not directly affect the expression of CD103 in CD4⁺ or CD8⁺ T cells *in vitro* (Figure 4b), indicating that ERB treatment increases CD103⁺ TILs through upregulating E-cadherin expression of tumor *in vivo*. To clarify the role of CD103 in the ERB-induced antitumor effects, we analyzed tumor growth in CD103-deficient mice. Tumor growth was enhanced in CD103-deficient mice compared to wildtype mice, and the ERB-induced antitumor effect was abolished in CD103-deficient

mice (Figure 4c). The ERB-induced E-cadherin expression was comparable between wildtype mice and CD103-deficient mice (Supplementary Figure S5). Combined, these results indicate that the ERB-induced antitumor effect is dependent on CD103.

3.5. CD103 is required for ERB-induced TIL activation

To clarify the mechanism of the antitumor effect of ERB via CD103, we evaluated the TIL number of CD103-deficient mice. The number of both CD4⁺ and CD8⁺ TILs was significantly lower in CD103-deficient mice than in the wildtype mice in the absence of ERB treatment (Figure 5a). Although ERB treatment increased the number of both CD4⁺ and CD8⁺ TILs in wildtype mice, this increase of the TIL number was not observed in CD103-deficient mice (Figure 5a). We also found

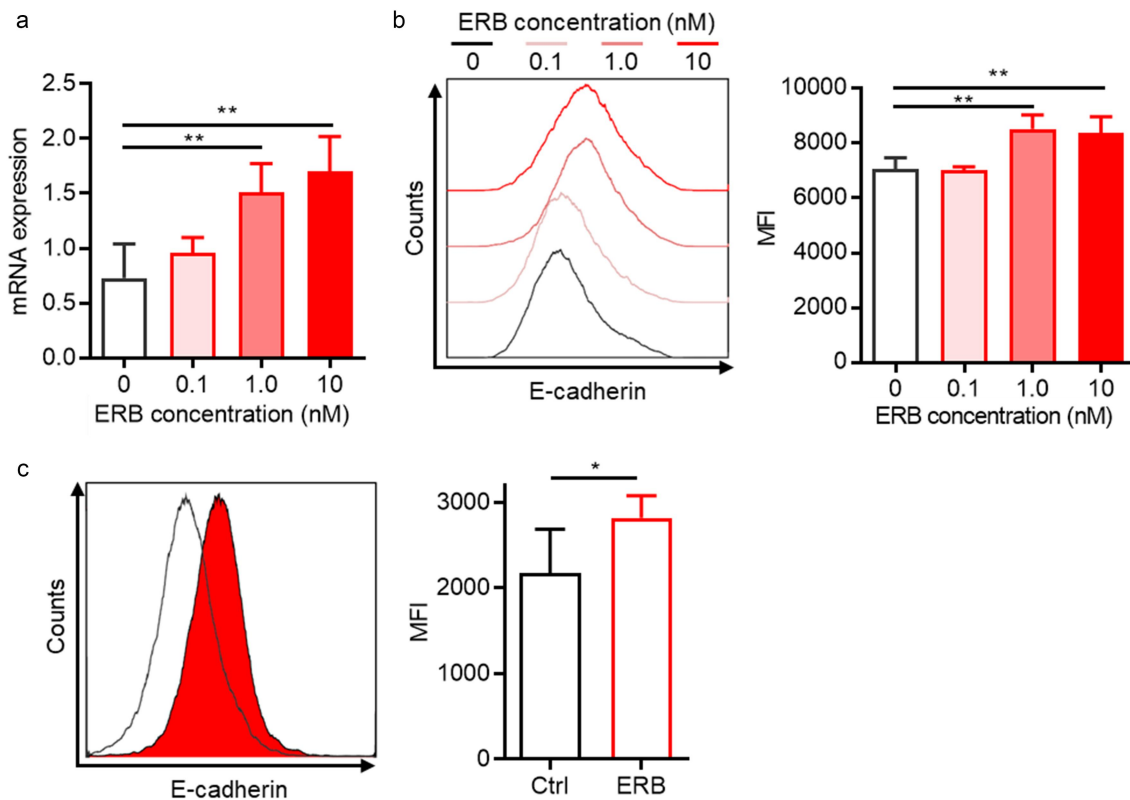


Figure 3. ERB enhanced the E-cadherin expression in MC38. Note: (A) Quantitative RT-PCR analysis of E-cadherin expression in MC38 stimulated with various concentrations of ERB for 24 hours ($n = 6$ per group). (B) Representative flow cytometric analysis and MFI of E-cadherin expression in MC38 with various concentrations of ERB for 3 days *in vitro* ($n = 6$ per group). (C) Representative flow cytometric analysis and MFI of E-cadherin expression in MC38 5 days after tumor inoculation with ERB administration on day 2 ($n = 6$ per group). Ctrl: control, ERB: eribulin mesylate, MFI: Mean fluorescence intensity. Error bars indicate ± 1 SED in (A), and ± 1 SD in (B and C); * $p < 0.05$, ** $p < 0.01$.

that expression of GZMB, LAG3 and Tim3 in CD8⁺ TILs and perforin expression in both CD4⁺ and CD8⁺ TILs were significantly lower in CD103-deficient mice than in wildtype mice in the absence of ERB treatment, although expression of CD38, CD69 and TIGIT in both CD4⁺ and CD8⁺ TILs was comparable (Figure 5b-d). Although ERB treatment increased the expression of the activation markers (CD38 and CD69), cytotoxic molecules (GZMB and perforin) and immune check point molecules (LAG3, Tim3 and TIGIT) in both CD4⁺ and CD8⁺ TILs in wildtype mice, such increased expression by ERB treatment was not observed in CD103-deficient mice (Figure 5b-d). These results suggest that CD103 is required for ERB-induced TIL activation.

4. Discussion

In our study, ERB increased the TIL number, as well as the expression of activation markers, inhibitory check-point molecules and cytotoxic molecules on TILs in the MC38 tumor mouse model. In addition, the ERB-induced antitumor effect was dependent on both CD4⁺ and CD8⁺ T cells. We also confirmed that ERB increased E-cadherin expression in MC38, LLC and MB49, but not in B16F10 or 4T1, and this was consistent with the ERB-induced anti-tumor effect in each tumor cell line, although poor immunogenicity in B16F10 and 4T1 may also be involved in the

resistance to ERB treatment. E-cadherin binds to CD103, and binding of E-cadherin to CD103 on T cells leads to an increased retention and subsequent induction of immunological synapse between T cells and tumor cells, which would result in T-cell activation characterized by secretion of cytokines and lytic granules^{24,25}. Indeed, ERB increased CD103⁺ TIL number in our study. Moreover, the ERB-induced antitumor effect with increased TIL number and expression of activation markers, cytotoxic molecules and inhibitory check point molecules on TILs was abrogated in CD103-deficient mice. Collectively, these results suggest that ERB induces retention, proliferation and activation of CD103⁺ TILs through upregulation of E-cadherin expression of tumor cells, and thereby exerts antitumor effects. Given that ERB induces ICD as shown above through increased extracellular ATP and HMGB1, ERB-induced ICD may also be involved in the enhancement of the immune response to tumors.

E-cadherin is regarded as a tumor suppressor molecule and a decrease in E-cadherin expression is associated with EMT. Since EMT leads to acquisition of invasive and metastatic abilities, the ERB-induced E-cadherin expression is suggested to inhibit cancer progression. Indeed, Kashiwagi et al analyzed E-cadherin expression before and after ERB treatment in advanced breast cancer patients and reported that all ERB responders showed increased E-cadherin

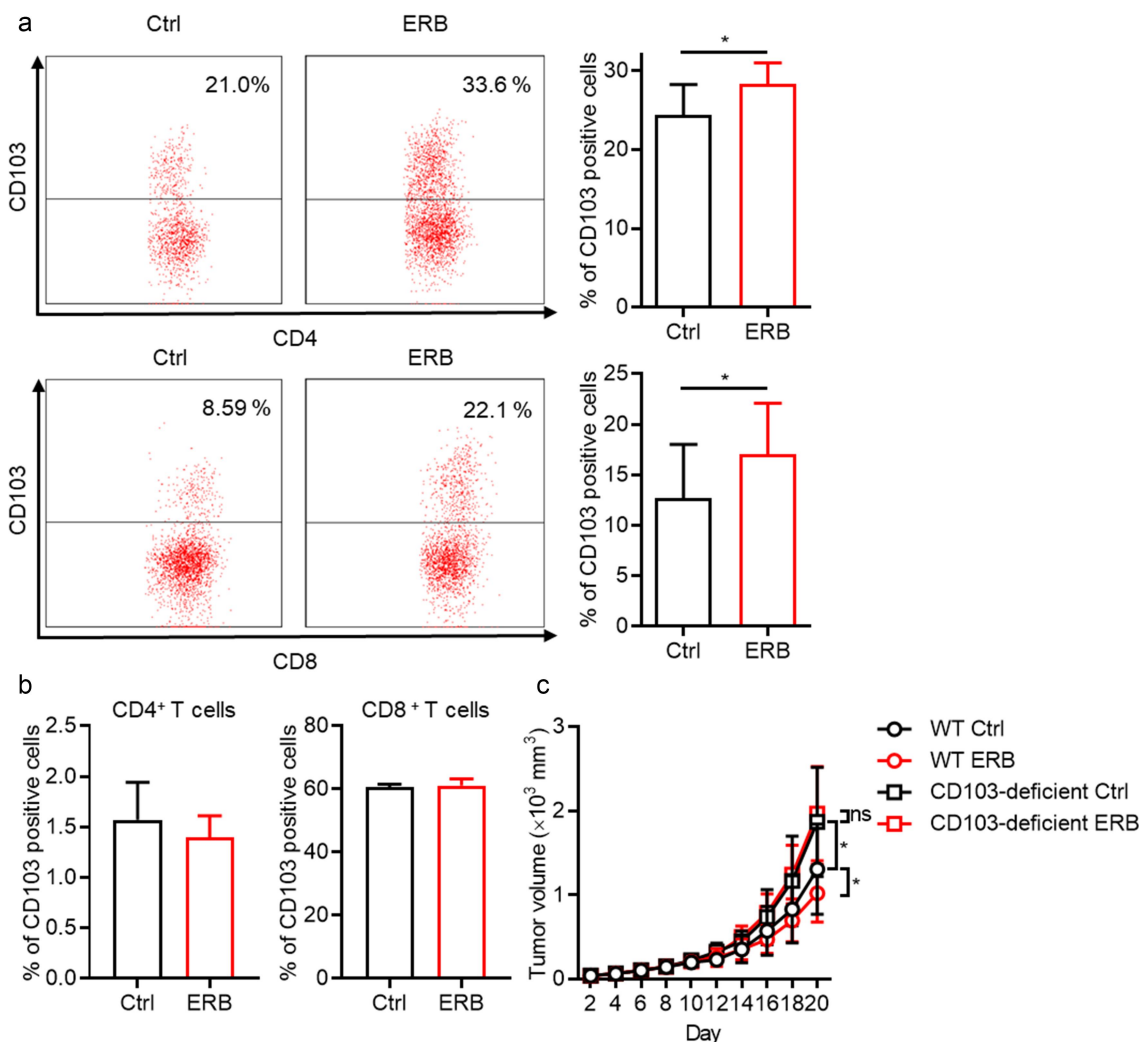


Figure 4. The ERB-induced antitumor effect is dependent on CD103. Note: (A) Representative flow cytometric analysis and proportion of CD103⁺ cells in CD4⁺ and CD8⁺ T cells in tumors 7 days after tumor inoculation with ERB administration on day 2 ($n = 11$ per group). (B) Proportion of CD103⁺ cells in CD4⁺ and CD8⁺ T cells of the murine spleen stimulated with ERB for 3 days ($n = 6$ per group). (C) Time course of the tumor volume after MC38 cells were intradermally inoculated into wildtype mice or CD103-deficient mice with ERB administration ($n = 19$ per group of wildtype mice, $n = 16$ in CD103-deficient mice with no treatment and $n = 17$ in CD103-deficient mice with ERB treatment). Ctrl: control, ERB: eribulin mesylate, ns: not significant. Error bars indicate ± 1 SD; * $p < 0.05$.

expression²⁶. However, our study suggests a novel mechanism of ERB-induced antitumor effect via interaction of increased E-cadherin expression with CD103 on TILs. Therefore, not only increased E-cadherin expression but also an increased number of CD103⁺ TILs, and the consequent increased expression of activation markers and cytotoxic molecules on TILs, might predict the outcome of patients treated with ERB.

Inhibitory immune checkpoint molecules are key regulators of the immune response to tumors. Recent clinical studies demonstrated that checkpoint inhibitors targeting inhibitory immune checkpoint molecules such as anti-PD-1 and anti-CTLA-4 antibodies improved prognosis of patients with various advanced tumors. However, the antitumor effect of immune checkpoint inhibitors remains unsatisfactory, and most patients do not obtain a complete response. Therefore, therapies involving

various combinations with immune checkpoint inhibitors have been tried. Given the immune modulatory effects of ERB treatment seen in our study, ERB may enhance the antitumor effect of immune checkpoint inhibitors. In addition, ERB treatment increased the expression of LAG3, TIGIT and Tim3, suggesting that ERB may induce not only activation but also exhaustion of TILs through increased expression of LAG3, TIGIT and Tim3. Therefore, although the combination of ERB with anti-PD-1 antibody did not show a stronger tumor response compared to anti-PD-1 antibody monotherapy in this study and a randomized clinical trial for patients with HER2-positive, ERBB-2 negative metastatic breast cancer demonstrated that the addition of pembrolizumab to ERB did not improve PFS or OS compared to ERB monotherapy²⁷, treatment targeting other molecules including LAG3, TIGIT and Tim3 combined with ERB

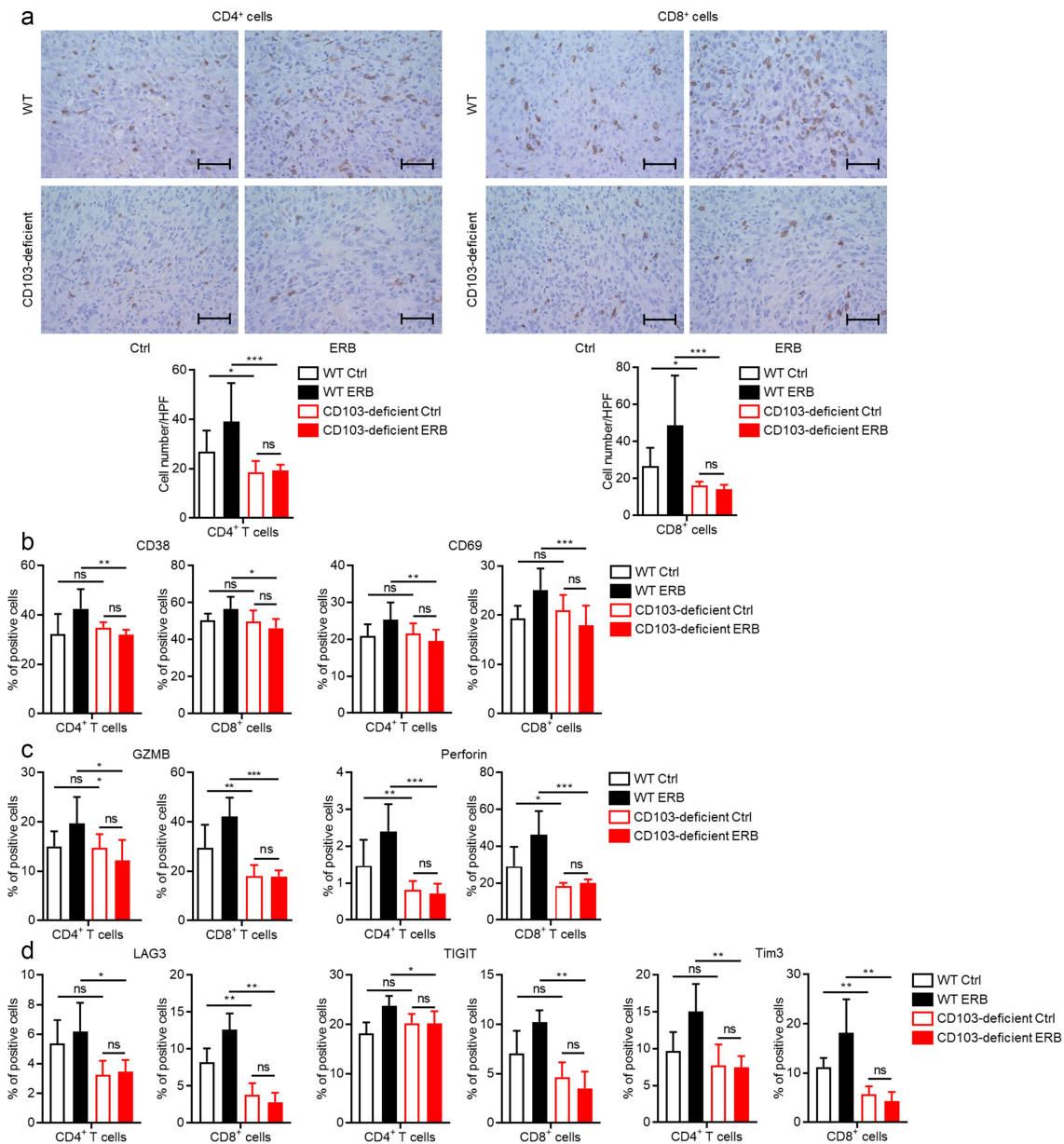


Figure 5. ERB not only increases T cells in the tumors but also activated T cells via CD103. Note: (A) Representative immunohistochemical studies and the number of CD4⁺ and CD8⁺ T cells in the tumor 10 days after the inoculation of MC38 into wildtype mice or CD103-deficient mice ($n = 12$ per group of wildtype mice, and $n = 6$ per group of CD103-deficient mice. Bar = 50 μ m). (B-D) Flow cytometric analysis of expression of CD38, CD69 (B), GZMB, perforin (C), LAG3, TIGIT, and Tim3 (D) in CD4⁺ and CD8⁺ T cells in tumors 7 days after tumor inoculation with ERB administration on day 2 into wildtype mice or CD103-deficient mice. ($n = 6$ [CD38 in each group, and GZMB and perforin in the CD103-deficient mice group], $n = 12$ [CD69 in each group, and GZMB and perforin in the wildtype mice group], and $n = 5$ [LAG3, Tim3, and TIGIT in each group]). WT: wildtype, Ctrl: control, ERB: Eribulin mesylate, LAG3: lymphocyte activation gene 3, TIGIT: T-cell immunoreceptor with Ig and ITIM domains, Tim3: T-cell immunoglobulin and mucin domain 3, GZMB: granzyme B, ns: not significant. Error bars indicate ± 1 SD; * $p < 0.05$, ** $p < 0.01$, *** $p < 0.001$.

might exert potent antitumor effects. Further basic and clinical studies are required for elucidating the efficacy of these combination treatments.

5. Conclusion

Our study indicates the antitumor effect of ERB due to the immune response induced by E-cadherin expression and the subsequent increased activation of CD103⁺ TILs. We believe that our study may provide the basis for future studies using

ERB in combination with other therapies including immune checkpoint inhibitors.

Acknowledgments

We thank Cosmin Florescu (Medical English Communications Center, University of Tsukuba) for his useful comments.

Disclosure statement

KO has received speaker's fees from Eisai for topics unrelated to this study. All other authors declare that they have no known competing financial interests

or personal relationships that could have appeared to influence the work reported in this paper.

Funding

This study was supported by Eisai Co., Ltd (Japan).

References

- Jimenez PC, Wilke DV, Costa-Lotufo LV. Marine drugs for cancer: surfacing biotechnological innovations from the oceans. *Clinics (Sao Paulo)*. 2018;73:e482s. doi:10.6061/clinics/2018/e482s.
- Cortes J, Schoffski P, Littlefield BA. Multiple modes of action of eribulin mesylate: emerging data and clinical implications. *Cancer Treat Rev*. 2018;70:190–198. doi:10.1016/j.ctrv.2018.08.008.
- Towle MJ, Salvato KA, Budrow J, Wels BF, Kuznetsov G, Aalfs KK, Welsh S, Zheng W, Seletsky BM, Palme MH, et al. In vitro and in vivo anticancer activities of synthetic macrocyclic ketone analogues of halichondrin B. *Cancer Res*. 2001;61:1013–1021.
- Kawano S, Asano M, Adachi Y, Matsui J. Antimitotic and non-mitotic effects of eribulin mesilate in soft tissue sarcoma. *Anticancer Res*. 2016;36:1553–1561.
- Yoshida T, Ozawa Y, Kimura T, Sato Y, Kuznetsov G, Xu S, Uesugi M, Agoulnik S, Taylor N, Funahashi Y, et al. Eribulin mesilate suppresses experimental metastasis of breast cancer cells by reversing phenotype from epithelial–mesenchymal transition (EMT) to mesenchymal–epithelial transition (MET) states. *Br J Cancer*. 2014;110:1497–1505. doi:10.1038/bjc.2014.80.
- Cortes J, O'Shaughnessy J, Loesch D, Blum JL, Vahdat LT, Petrakova K, Chollet P, Manikas A, Diéras V, Delozier T, et al. Eribulin monotherapy versus treatment of physician's choice in patients with metastatic breast cancer (EMBRACE): a phase 3 open-label randomised study. *Lancet*. 2011;377:914–923. doi:10.1016/S0140-6736(11)60070-6.
- Schöffski P, Chawla S, Maki RG, Italiano A, Gelderblom H, Choy E, Grignani G, Camargo V, Bauer S, Rha SY, et al. Eribulin versus dacarbazine in previously treated patients with advanced liposarcoma or leiomyosarcoma: a randomised, open-label, multicentre, phase 3 trial. *Lancet*. 2016;387:1629–1637. doi:10.1016/S0140-6736(15)01283-0.
- Fujisawa Y, Fujimura T, Matsushita S, Yamamoto Y, Uchi H, Otsuka A, Funakoshi T, Miyagi T, Hata H, Gosho M, et al. The efficacy of eribulin mesylate for patients with cutaneous angiosarcoma previously treated with taxane: a multicentre prospective observational study. *Br J Dermatol*. 2020;183:831–839. doi:10.1111/bjd.19042.
- Ito K, Hamamichi S, Abe T, Akagi T, Shiota H, Kawano S, Asano M, Asano O, Yokoi A, Matsui J, et al. Antitumor effects of eribulin depend on modulation of the tumor microenvironment by vascular remodeling in mouse models. *Cancer Sci*. 2017;108:2273–2280. doi:10.1111/cas.13392.
- Goto W, Kashiwagi S, Asano Y, Takada K, Morisaki T, Fujita H, Takashima T, Ohsawa M, Hirakawa K, Ohira M. Eribulin promotes antitumor immune responses in patients with locally advanced or metastatic breast cancer. *Anticancer Res*. 2018;38:2929–2938.
- Kashiwagi S, Asano Y, Goto W, Takada K, Takahashi K, Noda S, Takashima T, Onoda N, Tomita S, Ohsawa M, et al. Use of Tumor-infiltrating lymphocytes (TILs) to predict the treatment response to eribulin chemotherapy in breast cancer. *PLoS One*. 2017;12:e0170634. doi:10.1371/journal.pone.0170634.
- Kim Y, Shin Y, Kang GH. Prognostic significance of CD103+ immune cells in solid tumor: a systemic review and meta-analysis. *null*. 2019;9:3808. doi:10.1038/s41598-019-40527-4.
- Hardenberg JB, Braun A, Schön MP. A Yin and Yang in epithelial immunology: the roles of the α E(CD103) β 7 integrin in T cells. *J Invest Dermatol*. 2018;138:23–31. doi:10.1016/j.jid.2017.05.026.
- Abd Hamid M, Colin-York H, Khalid-Alham N, Browne M, Cerundolo L, Chen J-L, Yao X, Rosendo-Machado S, Waugh C, Maldonado-Perez D, et al. Self-maintaining CD103(+) cancer-specific T cells are highly energetic with rapid cytotoxic and effector responses. *Cancer Immunol Res*. 2020;8:203–216. doi:10.1158/2326-6066.CIR-19-0554.
- Franciszkievicz K, Le Floch A, Boutet M, Vergnon I, Schmitt A, Mami-Chouaib F. CD103 or LFA-1 engagement at the immune synapse between cytotoxic T cells and tumor cells promotes maturation and regulates T-cell effector functions. *Cancer Res*. 2013;73:617–628. doi:10.1158/0008-5472.CAN-12-2569.
- Djenidi F, Adam J, Goubar A, Durgeau A, Meurice G, de Montpréville V, Validire P, Besse B, Mami-Chouaib F. CD8 +CD103+ tumor-infiltrating lymphocytes are tumor-specific tissue-resident memory T cells and a prognostic factor for survival in lung cancer patients. *J Immunol*. 2015;194:3475–3486. doi:10.4049/jimmunol.1402711.
- Webb JR, Milne K, Watson P, deLeeuw RJ, Nelson BH. Tumor-infiltrating lymphocytes expressing the tissue resident memory marker CD103 are associated with increased survival in high-grade serous ovarian cancer. *Clin Cancer Res*. 2014;20:434–444. doi:10.1158/1078-0432.CCR-13-1877.
- Oya K, Nakamura Y, Zhenjie Z, Tanaka R, Okiyama N, Ichimura Y, Ishitsuka Y, Saito A, Kubota N, Watanabe R, et al. Combination treatment of topical imiquimod plus anti-PD-1 antibody exerts significantly potent antitumor effect. *Cancers (Basel)*. 2021;13:3948. doi:10.3390/cancers13163948.
- Zhong W, Myers JS, Wang F, Wang K, Lucas J, Rosfjord E, Lucas J, Hooper AT, Yang S, Lemon LA, et al. Comparison of the molecular and cellular phenotypes of common mouse syngeneic models with human tumors. *Bmc Genomics*. 2020;21:2. doi:10.1186/s12864-019-6344-3.
- Fucikova J, Kepp O, Kasikova L, Petroni G, Yamazaki T, Liu P, Zhao L, Spisek R, Kroemer G, Galluzzi L. Detection of immunogenic cell death and its relevance for cancer therapy. *Cell Death Dis*. 2020;11:1013. doi:10.1038/s41419-020-03221-2.
- Jiang X, Liu G, Li Y, Pan Y. Immune checkpoint: the novel target for antitumor therapy. *Genes Dis*. 2021;8:25–37. doi:10.1016/j.gendis.2019.12.004.
- Zhang X, Zhang H, Chen L, Feng Z, Gao L, Li Q. TIGIT expression is upregulated in T cells and causes T cell dysfunction independent of PD-1 and Tim-3 in adult B lineage acute lymphoblastic leukemia. *Cell Immunol*. 2019;344:103958. doi:10.1016/j.cellimm.2019.103958.
- Dybdal-Hargreaves NF, Risinger AL, Mooberry SL. Regulation of E-cadherin localization by microtubule targeting agents: rapid promotion of cortical E-cadherin through p130Cas/Src inhibition by eribulin. *Oncotarget*. 2018;9:5545–5561. doi:10.18632/oncotarget.23798.
- Floch AL, Jalil A, Vergnon I, Chansac BLM, Lazar V, Bismuth G, Chouaib S, Mami-Chouaib F. α E β 7 integrin interaction with E-cadherin promotes antitumor CTL activity by triggering lytic granule polarization and exocytosis. *J Exp Med*. 2007;204:559–570. doi:10.1084/jem.20061524.
- Morikawa R, Nemoto Y, Yonemoto Y, Tanaka S, Takei Y, Oshima S, Nagaishi T, Tsuchiya K, Nozaki K, Mizutani T, et al. Intraepithelial lymphocytes suppress intestinal tumor growth by cell-to-cell contact via CD103/E-Cadherin Signal. *Cell Mol Gastroenterol Hepatol*. 2021;11:1483–1503. doi:10.1016/j.jcmgh.2021.01.014.
- Kashiwagi S, Asano Y, Goto W, Takada K, Takahashi K, Hatano T, Tanaka S, Takashima T, Tomita S, Motomura H, Ohsawa M. Mesenchymal-epithelial transition and tumor vascular remodeling in eribulin chemotherapy for breast cancer. *Anticancer Res*. 2018;38:401–410.
- Tolaney SM, Barroso-Sousa R, Keenan T, Li T, Trippa L, Vaz-Luis I, Wulf G, Spring L, Sinclair NF, Andrews C, et al. Effect of eribulin with or without pembrolizumab on progression-free survival for patients with hormone receptor–positive, ERBB2–negative metastatic breast cancer. *JAMA Oncol*. 2020;6:1598–1605. doi:10.1001/jamaoncol.2020.3524.